

# STATIC AND DYNAMIC STRESS INTENSITY FACTORS OF BRANCHED CRACKS

Piotr Fedeliński<sup>1a</sup>, Mateusz Holek<sup>1b</sup>

<sup>1</sup>Institut Mechaniki i Inżynierii Obliczeniowej, Politechnika Śląska

<sup>a</sup>piotr.fedelinski@polsl.pl, <sup>b</sup>mateusz.holek@polsl.pl

## Summary

The boundary element method (BEM) is applied to analysis of static and dynamic stress intensity factors (SIF) of branched cracks. The numerical solution is obtained by discretization of external boundaries and crack surfaces. The problem of coincident crack boundaries is solved by the dual BEM in which for nodes on crack surfaces simultaneously the displacement and the traction boundary integral equations are applied. The dynamic problem is solved by using the Laplace transform method. Static stress intensity factors (SIF) are computed by the path independent J-integral and dynamic SIF by the crack opening displacement (COD) method. Numerical examples of a single crack and two interacting branched cracks in rectangular plates are presented. The influences of dimensions and shapes of voids in the centers of the branched cracks and the orientations and distances between two interacting cracks on SIF are analyzed.

**Keywords:** fracture, crack, stress intensity factors (SIF), boundary element method (BEM), Laplace transform method

## STATYCZNE I DYNAMICZNE WSPÓŁCZYNNIKI INTENSYWNOŚCI NAPRĘŻEŃ PEKNIĘĆ ROZGAŁĘZIONYCH

### Streszczenie

Zastosowano metodę elementów brzegowych (MEB) do analizy statycznych i dynamicznych współczynników intensywności naprężeń (WIN) pęknięć rozgałęzionych. Rozwiązanie numeryczne otrzymano w wyniku dyskretyzacji brzegów zewnętrznych tarczy i krawędzi pęknięć. Zastosowano sformułowanie dualne MEB do analizy pokrywających się krawędzi pęknięcia, w którym stosuje się jednocześnie dla węzłów pęknięcia brzegowe równanie całkowite przemieszczeń i sił powierzchniowych. Zagadnienie dynamiczne analizowano metodą transformacji Laplace'a. Statyczne współczynniki intensywności naprężeń (WIN) obliczono za pomocą J-całki niezależnej od konturu całkowania, a dynamiczne WIN na podstawie rozwarcia krawędzi pęknięcia. Przedstawiono przykłady numeryczne pojedynczego pęknięcia i dwóch oddziałujących pęknięć rozgałęzionych w tarczach. Badano wpływ wielkości i kształtu pustek w środku pęknięcia rozgałęzionego oraz orientacji i odległości między dwoma pęknięciami na WIN.

**Słowa kluczowe:** pęknięcie, szczelina, współczynniki intensywności naprężeń (WIN), metoda elementów brzegowych (MEB), metoda transformacji Laplace'a

### 1. INTRODUCTION

Some materials can contain branched cracks as a result of technological processes or dynamic fracture. For example, during the process of sintering small voids remain at corners of fibers with branched cracks growing

from the pores. Fast running cracks subjected to high loadings can split into several branches. The stresses at crack tips of branched cracks are characterized by stress intensity factors (SIF). The values of static or dynamic

SIF for a general geometry of the body and loading conditions are obtained by numerical methods.

Daux et al. [1] presented the extended finite element method (X-FEM) to analysis of cracks with multiple branches and cracks emanating from holes. A standard displacement approximation was enriched by incorporating additional discontinuous functions. The method allows the modelling of discontinuities independently of the mesh. Fedeliński [7] analyzed sintered materials with branched cracks growing from the voids situated at corners of fibers. The material was modelled as a two-dimensional linear-elastic structure using the boundary element method (BEM). The materials without voids and with voids having different shapes were considered. The influence of lengths of cracks and shapes of voids on SIF and effective elastic properties (the Young modulus and the Poisson ratio) were studied. The overall properties of the sintered materials were determined by considering the representative volume element (RVE) with large number of branched cracks. The sensitivity of effective elastic properties on boundary conditions imposed on the RVE was studied.

Raffie et al. [9] investigated bifurcation and trifurcation of fast running cracks under various biaxial loading conditions. Arbitrary curvilinear crack propagations were analyzed by the time-domain BEM. Branching of cracks was controlled by the opening mode SIF and velocity and direction of crack growth by the maximum circumferential stress at the crack tip. Numerical solutions were compared with experimental results. Fedeliński [6] applied the boundary element method to analysis of statically and dynamically loaded plates with branched and intersecting cracks. The dynamic problem was solved by using the Laplace transform method and the solution in the time domain was computed by the Durbin numerical inversion method. Numerical examples of a branched crack in a rectangular plate and a star-shaped crack in a square plate were presented. The influences of angles between branches of the crack and dimensions of the plate for the star-shaped crack on dynamic SIF were analyzed.

In the present work the boundary element method is applied to analysis of static and dynamic stress intensity factors of branched cracks in rectangular plates. The crack problem is solved by the dual BEM which was developed for static loading by Portela et al. [8] and for dynamic loading by Fedeliński et al. [2]. An overview of different BEM approaches in dynamic fracture mechanics was presented by Fedeliński [3], [4], [5]. The present paper is an extension of the previous work [6] published by the author. In this work new numerical examples of a single crack and two interacting branched cracks in rectangular plates are presented.

## 2. LAPLACE TRANSFORM BOUNDARY ELEMENT METHOD

The solution of dynamic problems by the Laplace transform boundary element method was presented in detail by Fedeliński et al. in [2]. Here for the completeness of the paper the method is briefly described.

Consider a homogeneous and isotropic linear elastic body enclosed by a boundary  $\Gamma$ . For a body which is not subjected to body forces and which has zero initial displacements and velocities, the Laplace transform of the displacements of points  $x'$  and  $x''$  on smooth crack surfaces, can be represented by the following boundary integral equation

$$\frac{1}{2}\bar{u}_i(x',s) + \frac{1}{2}\bar{u}_i(x'',s) = \int_{\Gamma} \bar{U}_{ij}(x',x,s)\bar{t}_j(x,s)d\Gamma(x) - \int_{\Gamma} \bar{T}_{ij}(x',x,s)\bar{u}_j(x,s)d\Gamma(x), \quad (1)$$

where  $\bar{U}_{kij}(x',x,s)$ ,  $\bar{T}_{ij}(x',x,s)$  are the Laplace transforms of fundamental solutions of elastodynamics,  $\bar{u}_j(x,s)$ ,  $\bar{t}_j(x,s)$  are the Laplace transforms of the displacements and tractions respectively, at the boundary,  $s$  is the integral transform parameter. The Laplace transform of the traction equation for points which belong to smooth crack surfaces is

$$\frac{1}{2}\bar{t}_j(x',s) - \frac{1}{2}\bar{t}_j(x'',s) = n_k(x') \left[ \int_{\Gamma} \bar{U}_{kij}(x',x,s)\bar{t}_k(x,s)d\Gamma(x) - \int_{\Gamma} \bar{T}_{kij}(x',x,s)\bar{u}_k(x,s)d\Gamma(x) \right], \quad (2)$$

where  $\bar{U}_{kij}(x',x,s)$  and  $\bar{T}_{kij}(x',x,s)$  are the Laplace transforms of other fundamental solutions of elastodynamics.

The numerical solution of a general mixed-mode crack problem is obtained after discretizing boundary quantities. The boundary  $\Gamma$  of the body is divided into boundary elements. Quadratic elements are used for the discretization of the boundary. The displacements and tractions are interpolated using: continuous elements for the external boundary and discontinuous elements on the crack faces. Displacements and tractions are approximated within each element using interpolation functions. A distinct set of boundary integral equations is obtained by applying the displacement equation for nodes along the external boundary and along the crack and the traction equation for the nodes along the crack. The set of discretized boundary integral equations can be written in matrix form as

$$\bar{H}\bar{u} = \bar{G}\bar{t}, \quad (3)$$

where  $\bar{\mathbf{u}}$  and  $\bar{\mathbf{t}}$  contain nodal values of the transformed displacements and tractions respectively, and  $\bar{\mathbf{H}}$  and  $\bar{\mathbf{G}}$  depend on integrals of the transformed fundamental solutions and the interpolating functions. The matrices  $\bar{\mathbf{H}}$  and  $\bar{\mathbf{G}}$  are reordered according to the boundary conditions to give new matrices  $\bar{\mathbf{A}}$  and  $\bar{\mathbf{B}}$ . The matrix  $\bar{\mathbf{A}}$  is multiplied by the vector  $\bar{\mathbf{x}}$  of unknown transformed displacements and tractions and  $\bar{\mathbf{B}}$  by the vector  $\bar{\mathbf{y}}$  of the known transformed boundary conditions, as follows

$$\bar{\mathbf{A}}\bar{\mathbf{x}} = \bar{\mathbf{B}}\bar{\mathbf{y}} \quad (4)$$

or

$$\bar{\mathbf{A}}\bar{\mathbf{x}} = \bar{\mathbf{f}}, \quad (5)$$

where  $\bar{\mathbf{f}} = \bar{\mathbf{B}}\bar{\mathbf{y}}$  is a known vector. The matrix equation (5) is solved giving the unknown transformed displacements and tractions for a particular integral transform parameter. For a simple temporal variation of the prescribed boundary conditions their integral transforms can be calculated analytically. In order to obtain the unknown displacements and tractions as functions of time, the unknown transformed variables must be computed for a series of parameters. The final time-dependent solution can be obtained from the numerical Durbin inversion.

### 3. NUMERICAL EXAMPLES

Two numerical examples are considered: a single branched crack with a void in the center and two branched cracks in rectangular plates. The material of the plates has the following mechanical properties: the Young modulus  $E=200$  GPa, the Poisson ratio  $\nu=0.3$ , mass density  $\rho=8000$  kg/m<sup>3</sup> and the plate is in the plane strain conditions. The plates are loaded statically and dynamically by the Heaviside time dependent uniformly distributed tractions  $p$  applied at the initial time  $t=0$ . The numerical solutions are obtained using 50 Laplace parameters and the time step is  $\Delta t=0.2$   $\mu$ s. Static SIF are computed using the path independent J-integral and the dynamic SIF using crack opening displacements.

#### 3.1. SINGLE BRANCHED CRACK WITH A VOID IN THE CENTER

The crack having the length  $a=1$  cm is in the center of the rectangular plate of width  $2w$  and the height  $2h$  and the ratio of dimensions is  $h/w=4/5$  and  $a/w=0.5$ , as shown in Fig. 1. The branches are inclined at the angle  $\alpha=\pi/3$  rad. Two horizontal edges of the plate are loaded in the vertical direction. The following cases are considered: a branched crack without a void (Fig. 1a), with a triangular void (Fig. 1b) and with a circular void (Fig. 1c) in the center. Two dimensions of the void  $r$  are

studied  $r/a=0.25$  (called small) and  $0.50$  (called large). The plate with the branched crack is divided into 140 boundary elements and the plates with the crack and the void into 128 boundary elements (80 elements for the external boundary and the remaining elements for the crack and the void). The stress intensity factors are normalized with respect to the SIF  $K_o = p\sqrt{\pi c}$ , where  $2c$  is the width of the crack in the horizontal direction (Fig. 1a).

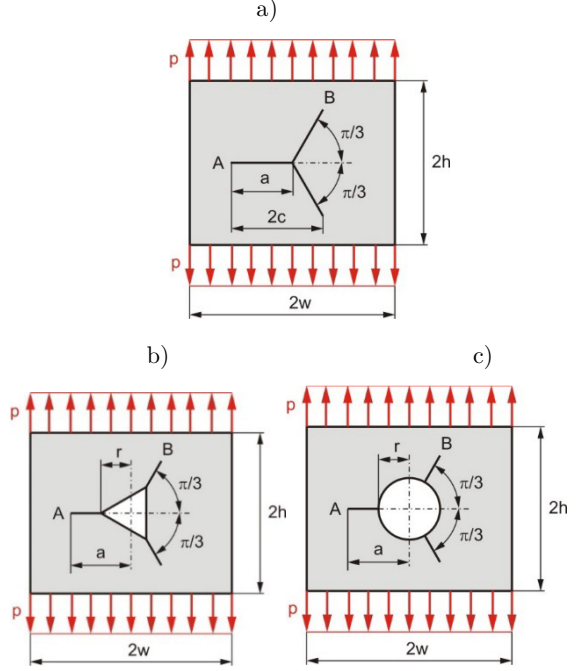


Fig.1. Single branched crack in a rectangular plate: (a) crack without a void, (b) crack with a triangular void, c) crack with a circular void in the center

Initially the plate is subjected to the static loading. The computed normalized SIF for the crack tips A and B are presented in Table 1. In Fig. 2 the initial and the deformed shapes are shown. The voids in the center of the crack, except the large circular void, have a small influence on the static SIF. The large circular void increases  $K_I(A)/K_o$  by 12.5 % and decreases  $K_I(B)/K_o$  by 10.8 % and  $K_{II}(B)/K_o$  by 10.5%.

Table 1. Static normalized SIF of the single branched crack

void	$K_I(A)/K_o$	$K_I(B)/K_o$	$K_{II}(B)/K_o$
without	1.530	0.444	0.914
triangular small	1.539	0.446	0.916
circular small	1.553	0.445	0.909
triangular large	1.554	0.442	0.902
circular large	1.721	0.396	0.818

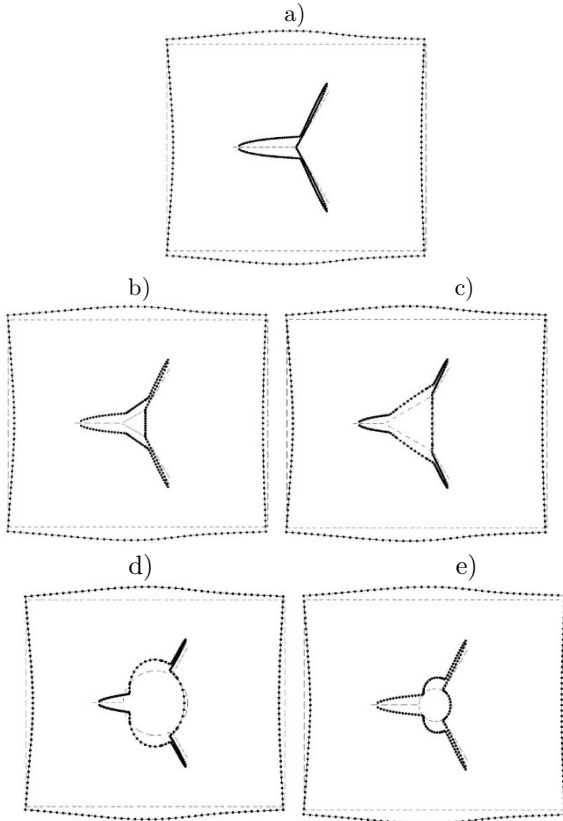


Fig. 2. Initial (dashed line) and deformed (continuous line) shape of the plate: (a) crack without the void, (b) crack with the small triangular void, (c) crack with the large triangular void, (d) crack with the small circular void, (e) crack with the large circular void

The normalized dynamic SIF for the crack with the large triangular and large circular void are presented in Fig. 3 and 4, respectively. The results for the small voids are not shown because of small influence of voids on DSIF. Initially when the longitudinal wave travels from the loaded boundary to the crack tips the DSIF are zero. The DSIF for the crack tip A are larger than for the crack tip B. The maximum values of dynamic DSIF are approximately two times larger than the corresponding static values of SIF. The large triangular void has small influence on DSIF and the large circular void increases  $K_I(A)/K_0$  and decreases  $K_I(B)/K_0$  and  $K_{II}(B)/K_0$ . Similar behavior is observed for the static loading.

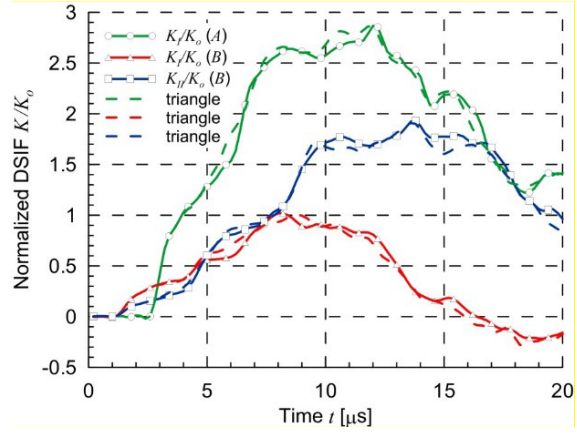


Fig.3. Normalized dynamic SIF for the branched crack with the large triangular void

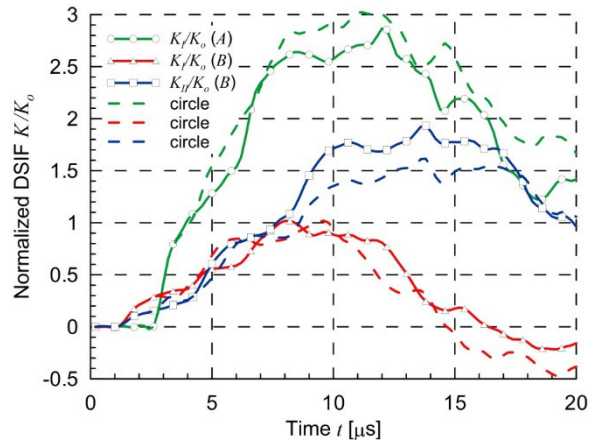
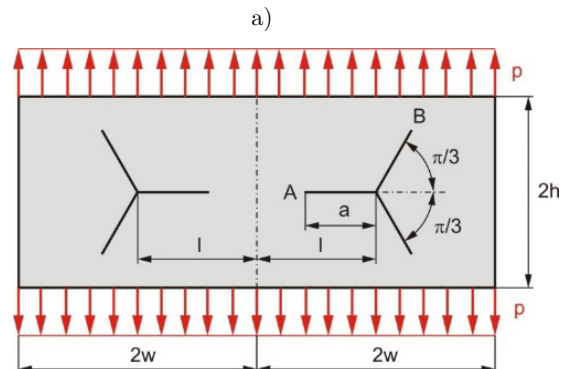


Fig. 4. Normalized dynamic SIF for the branched crack with the large circular void

### 3.2. TWO INTERACTING BRANCHED CRACKS

Two interacting branched cracks in a rectangular plate are considered. The dimensions of the crack and the plate, material properties and loading are the same as in the previous example. Two different orientations of the cracks and different distances between crack centers  $l/a=1.5, 2.0$  and  $2.5$  are considered, as shown in Fig. 5. Because of symmetry of the structures only one half of the plates with appropriate boundary conditions along the lines of symmetry are considered. The number of boundary elements and parameters of the Laplace method are the same as in the previous example.



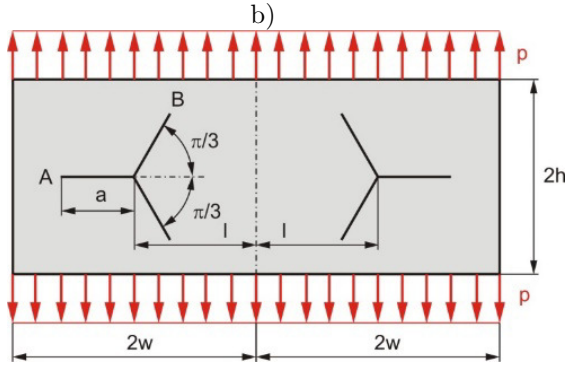


Fig. 5. Two interacting branched cracks: (a) interaction of horizontal branches, (b) interaction of inclined branches

The static stress intensity factors for two orientations of cracks and different distances between crack centers are given in Table 2 and 3.

Table 2. Static normalized SIF for the horizontal interacting branches

$l/a$	$K_I(A)/K_o$	$K_I(B)/K_o$	$K_{II}(B)/K_o$
1.5	1.435	0.432	0.745
2.0	1.383	0.410	0.805
2.5	1.435	0.386	0.855

Table 3. Static normalized SIF for the interacting inclined branches

$l/a$	$K_I(A)/K_o$	$K_I(B)/K_o$	$K_{II}(B)/K_o$
1.5	1.479	0.513	0.827
2.0	1.510	0.493	0.880
2.5	1.541	0.489	0.910

Two factors have an influence on stress intensity factors: interaction of cracks and interaction of cracks with the free vertical edges of the plate. When the distance between the cracks is increased the  $K_I(B)/K_o$  is decreased and  $K_{II}(B)/K_o$  is increased and  $K_I(A)/K_o$  is increased in the second configuration of cracks. The values of SIF for the second orientation of cracks are larger. In Table 2 the relative variation of  $K_I(A)/K_o$  is 3.6 %, for  $K_I(B)/K_o$  is 11.2 % and for the  $K_{II}(B)/K_o$  is 13.7 %. In Table 3 the relative variation of  $K_I(A)/K_o$  is 4.1 %, for  $K_I(B)/K_o$  is 4.9 % and for the  $K_{II}(B)/K_o$  is 9.4 %.

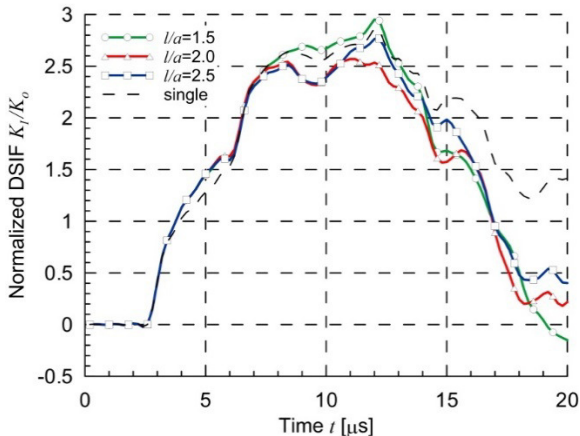


Fig. 6. Dynamic normalized SIF  $K_I(A)/K_o$  for the horizontal interacting branches

The dynamic SIF  $K_I(A)/K_o$  for the horizontal interacting branches for different distances between the cracks are compared with the solution for the single crack in Fig. 6. The distance between the cracks has a small influence on DSIF. The DSIF for the interacting cracks are smaller than the DSIF for the single crack at later times.

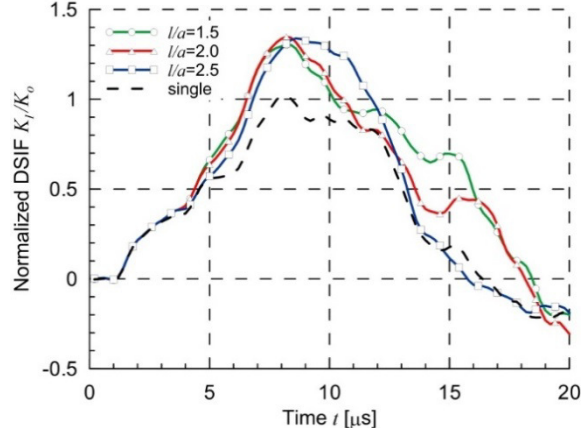


Fig. 7. Dynamic normalized SIF  $K_I(B)/K_o$  for the interacting inclined branches

The dynamic SIF  $K_I(B)/K_o$  for the interacting inclined branches for different distances between the cracks are compared with the solution for the single crack in Fig. 7. The maximum values of DSIF are similar for different distances between the cracks and are higher than the values for the single crack. At later times, the DSIF decrease with an increasing distance between the cracks. The cracks behave similar for static loading (see Table 3).

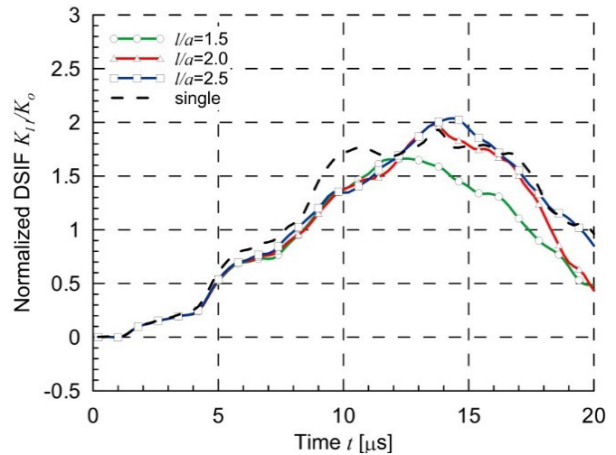


Fig. 8. Dynamic normalized SIF  $K_{II}(B)/K_o$  for the interacting inclined branches

The dynamic SIF  $K_{II}(B)/K_o$  for the inclined interacting branches for different distances between the cracks are compared with the solution for the single crack in Fig. 8. At later times, the DSIF increase with an increasing distance between the cracks. The cracks behave similar for the static loading (see Table 3).

#### 4. CONCLUSIONS

The solutions obtained by the Laplace transform BEM are stable. The maximum values of dynamic SIF are about two times larger than the static SIF. The voids in the center of the branched crack have small influence on static and dynamic stress intensity factors. The large circular void increases static SIF by less than 13%. For the interacting cracks when the distance between cracks is increased the opening mode SIF decrease, while the sliding mode SIF increase for the inclined branches. The

relative variations of static SIF do not exceed 14% for the considered orientations and distances between branched cracks.

Acknowledgement: The scientific research is financed by National Science Centre, Poland in years 2016-2019, grant no. 2015/19/B/ST8/02629.

#### Literature

1. Daux Ch., Moes N., Dolbow J., Sukumar N., Belytschko T.: Arbitrary branched and intersecting cracks with the extended finite element method. "International Journal for Numerical Methods in Engineering" 2000, Vol. 48, p. 1741-1760.
2. Fedeliński P., Aliabadi M. H., Rooke D.P.: The Laplace transform DBEM method for mixed-mode dynamic crack analysis. "Computers and Structures" 1996, Vol. 59, p. 1021-1031.
3. Fedeliński P.: Metoda elementów brzegowych w analizie dynamicznej układów odkształcalnych z pęknięciami, ZN Pol.Śl. s. „Mechanika”, z. 137, Gliwice 2000.
4. Fedeliński P.: Boundary element method in dynamic analysis of cracks. "Engineering Analysis with Boundary Elements" 2004, Vol. 28, p. 1135-1147.
5. Fedeliński P.: Metoda elementów brzegowych w dynamice układów odkształcalnych. Gliwice: Wyd. Pol. Śl., 2016. Monografia, nr 622.
6. Fedeliński P.: Dynamically loaded branched and intersecting cracks. "Journal of Civil Engineering, Environment and Architecture" 2017, Vol. 34, p. 17-26
7. Fedeliński P.: Effective elastic properties of sintered materials with branched cracks. In: AIP Conference Proceedings 1922, 2018, p. 030008-1-8.
8. Portela A., Aliabadi M. H., Rooke D. P.: The dual boundary element method: effective implementation for crack problems. "International Journal for Numerical Methods in Engineering" 1992, Vol. 33, p. 1269-1287.
9. Raffie S., Seelig Th., Gross D.: Simulation of dynamic crack curving and branching under biaxial loading by a time domain boundary integral equation method. "International Journal of Fracture" 2003, Vol. 120, p. 545-561.



Artykuł dostępny na podstawie licencji Creative Commons Uznanie autorstwa 3.0 Polska.  
<http://creativecommons.org/licenses/by/3.0/pl>